The influence of coating structure on micromachine stiction

J.G. Kushmerick [a], M.G. Hankins [b], M.P. de Boer [c], P.J. Clews [b], R.W. Carpick [a,*] and B.C. Bunker [a]

[a] *Biomolecular Materials and Interfaces 1140, MS 1413, Sandia National Laboratories, Albuquerque, NM 87185, USA*
[b] *MDL Operations 1746, MS 1084, Sandia National Laboratories, Albuquerque, NM 87185, USA*
[c] *Intelligent Micromachining 1749, MS 1080, Sandia National Laboratories, Albuquerque, NM 87185, USA*

Stiction and friction in micromachines is commonly inhibited through the use of silane coupling agents such as 1H-, 1H-, 2H-, 2H-perfluorodecyltrichlorosilane (FDTS). FDTS coatings have allowed micromachine parts processed in water to be released without debilitating capillary adhesion occurring. These coatings are frequently considered as densely-packed monolayers, well-bonded to the substrate. In this paper, it is demonstrated that FDTS coatings can exhibit complex nanoscale structures, which control whether micromachine parts release or not. Surface images obtained via atomic force microscopy reveal that FDTS coating solutions can generate micellar aggregates that deposit on substrate surfaces. Interferometric imaging of model beam structures shows that stiction is high when the droplets are present and low when only monolayers are deposited. As the aggregate thickness (tens of nanometers) is insufficient to bridge the 2 μm gap under the beams, the aggregates appear to promote beam–substrate adhesion by changing the wetting characteristics of coated surfaces. Contact angle measurements and condensation figure experiments have been performed on surfaces and under coated beams to quantify the changes in interfacial properties that accompany different coating structures. These results may explain the irreproducibility that is often observed with these films.

KEY WORDS: thin films; MEMS; adhesion; self-assembled monolayers; FDTS

1. Introduction

Adhesion between microstructures is a major failure mechanism for microelectromechanical (MEMS) devices. "Stiction" can occur either during the final steps of fabrication (release stiction) or when parts come into direct contact due to out-of-range inputs or mechanical instabilities (in-use stiction). The focus of this paper is on release stiction, in which capillary forces associated with processing fluids cause microstructures to be pulled into contact with the underlying substrate [1]. One strategy for minimizing release stiction involves applying hydrophobic coatings such as octadecyltrichlorosilane (OTS) or 1H-, 1H-, 2H-, 2H-perfluorodecyltrichlorosilane (FDTS) to all surfaces having access to organic coating solutions [2]. Replacement of the organic fluids with water then produces a condition in which the fluid no longer wets machine components, minimizing capillary forces below the level needed to pull compliant structures into contact. Both OTS and FDTS have the added benefits of reducing in-use stiction, friction, and wear, with FDTS exhibiting lower adhesion [3].

While films formed from silane coupling agents can exhibit excellent anti-stiction characteristics, film properties have been shown to be highly sensitive to processing parameters such as deposition time, temperature, the water content of the solution, concentration, and even what container the films are processed in [4,5]. Previous studies have indicated that one source of irreproducible behavior is that silane coating solutions do not always form ideal monolayers, but can produce a range of ordered surfactant structures including aggregated inverse micelles and multi-layer lamellar phases [5,6]. In some instances, structures such as the inverse micelles are formed and deposited directly from the coating solution. It appears that similar structures can also form by exposing well-ordered self-assembled monolayers to humid environments, promoting molecular reorganizations within the FDTS layer [7]. The purpose of this investigation is to determine if there is a direct correlation between the structure of the FDTS coatings and release stiction.

* Current address: Department of Engineering Physics, University of Wisconsin-Madison, 543 Engineering Research Building, 1500 Engineering Drive, Madison, WI 53706, USA.

2. Experimental

Reagents and solvents, including FDTS (Lancaster), isopropanol, and isooctane were used as-received without further purification. Substrate materials consisted of Si (100) single crystal wafers and micromachined cantilever beams. The micromachined structures were fabricated using the four-layer SUMMiT (Sandia Ultra-planar, Multi-level MEMS Technology) process involving the alternate deposition of polysilicon layers and sacrificial oxide layers (removed via a controlled time HF etch) [8]. All samples were transferred to deionized water, immersed in hydrogen peroxide to form a thin surface oxide, and immersed back in deionized water. The Si(100) samples were cleaned in a dilute ammonium hydroxide solution and rinsed with deionized water prior to coating.

Samples were exposed to the coating solution of 1 mM FDTS in isooctane. Once coated, samples were taken through a rinse sequence to replace isooctane by water and air-dried. Suspended cantilever beam test structures and unpatterned Si wafers were coated at the same time in a given

1023-8883/01/0300-0103$19.50/0

FDTS coating solution. Below, it is assumed that coating structures of Si(100) and polysilicon beams processed in parallel are identical. However, differences between the morphology and surface chemistry of Si(100) and polysilicon could conceivably modify FDTS coatings in ways that have not been anticipated.

Quantitative values for release stiction were obtained by examining the deflections of the cantilever beam test structures using interferometric microscopy [9]. Interference fringes of 547 nm green light were used to measure out of plane beam deflections vs. position with an absolute deflection accuracy of 10 nm across an entire beam. An analysis of the interference fringes is then used to calculate the crack length (distance from the beam support to the point where the beam contacts the substrate). If the dimensions and mechanical properties of the beam are known, the crack length can then be used to calculate the adhesion energy between the beam and the substrate in mJ/m^2.

Morphologies of FDTS-coated surfaces were obtained using a Digital Instruments Nanoscope III operated in the tapping mode. Film thicknesses were calculated with a Rudolph AutoEL II ellipsometer using a well-established three-layer (air, monolayer, substrate) model with an assumed refractive index of 1.45 for the FDTS film [10]. Surface hydrophobicity was measured using contact angle measurements made with a custom-built apparatus based on capillary rise on a vertical plate [11]. A Leica MZ6 stereomicroscope was used to determine the water level and to view the water meniscus. Images were captured by a charge-coupled device (CCD) camera into a Macintosh computer and digitally analyzed using a standard image processing program to determine contact angle values.[1]

Qualitative estimates of the relative hydrophobicity of coated surfaces under test beam structures were obtained using condensation figures. To make the measurements, beams were first mechanically removed using a micromanipulation stage and a Leica MZ6 stereomicroscope. Then, optical micrographs were obtained for the sample. After removal of the beams, test structures were exposed to supersaturated air to create a condition where water condensed on the surface. Condensation figures were then obtained by capturing optical micrographs of the condensed droplets on the sample surface. All images were captured via a CCD camera connected to a Macintosh computer.

3. Results and discussion

The overall test methodology used in this investigation involved first examining FDTS-coated polysilicon test samples in the interferometric optical microscope to determine the magnitude of release stiction. Sample batches with both low and high stiction were identified. Next tapping mode AFM was performed on the Si(100) wafers that were coated in parallel with the test structures to determine the FDTS film morphology. Finally, contact angle and condensation figure measurements were performed in an attempt to establish mechanisms to explain observed correlations between coating morphology and stiction.

3.1. Stiction measurements on cantilever beams

The significant batch-to-batch variations that are sometimes seen in the adhesion behavior of test beams coated with FDTS are illustrated in figure 1. Some test structures (figure 1(A)) exhibit very few interference fringes indicating that all beams have been released and are freely supported above the substrate.[2] Adhesive interactions are too small to bring the beams into contact with the substrate, and are certainly less than 0.01 mJ/m^2. In contrast, other test structures contain beams (figure 1(B)) that have all been pulled down to the underlying substrate due to the capillary forces during the drying process. The range in the crack length for the beams shown corresponds to a calculated range in adhesion energies of 0.15–3.1 mJ/m^2 [9,12]. Adhesion energies as high as 18 mJ/m^2 have been observed on some of the FDTS-coated test structures. The adhesion is almost as high as adhesion energies measured for similar test structures in the absence of a coating (20 mJ/m^2) due to the strong capillary forces during the drying process [13].

3.2. Coating morphologies

Tapping-mode AFM images of Si wafers coated in parallel with the test structures show that there are dramatic differences between the morphologies of FDTS coatings that cause the beams to stick and those that do not. Wafers corresponding to the non-adherent beams consist of monolayer coverages of FDTS (figure 2(A)). Ellipsometry measurements indicate that the films are 1.3 nm thick, which compares favorably with the 1.5 nm expected for a well-organized, densely packed monolayer with the fluorocarbon chains oriented perpendicular to the substrate. In contrast, Si wafers that correspond to adherent test structures are covered with aggregates of FDTS inverse micelles [5]. The aggregates appear as droplets that are several hundred nanometers in diameter and tens of nanometers thick (figure 2 (B) and (C)). Ellipsometry measurements of the film give an average film thickness of 2.6 nm, indicating that the aggregates account for at least 50% of the mass deposited (even if a monolayer of FDTS underlies the aggregates).

Variations in the fraction of the surface covered by FDTS aggregates appear to account for the greater than four-orders-of-magnitude range seen in the adhesion energy of test structures (figure 3). Although there is considerable scatter at high adhesion energies, it appears that higher aggregate concentrations result in greater release stiction.

[1] Analysis performed using the public domain NIH Image program (developed at the US National Institutes of Health and available on the Internet at http://rsb.info.nih.gov/nih-image/).

[2] The broad interference fringes seen on some of the beams in figure 1(A) are indicative of residual stress in the polysilicon that causes the beams to bend up slightly.

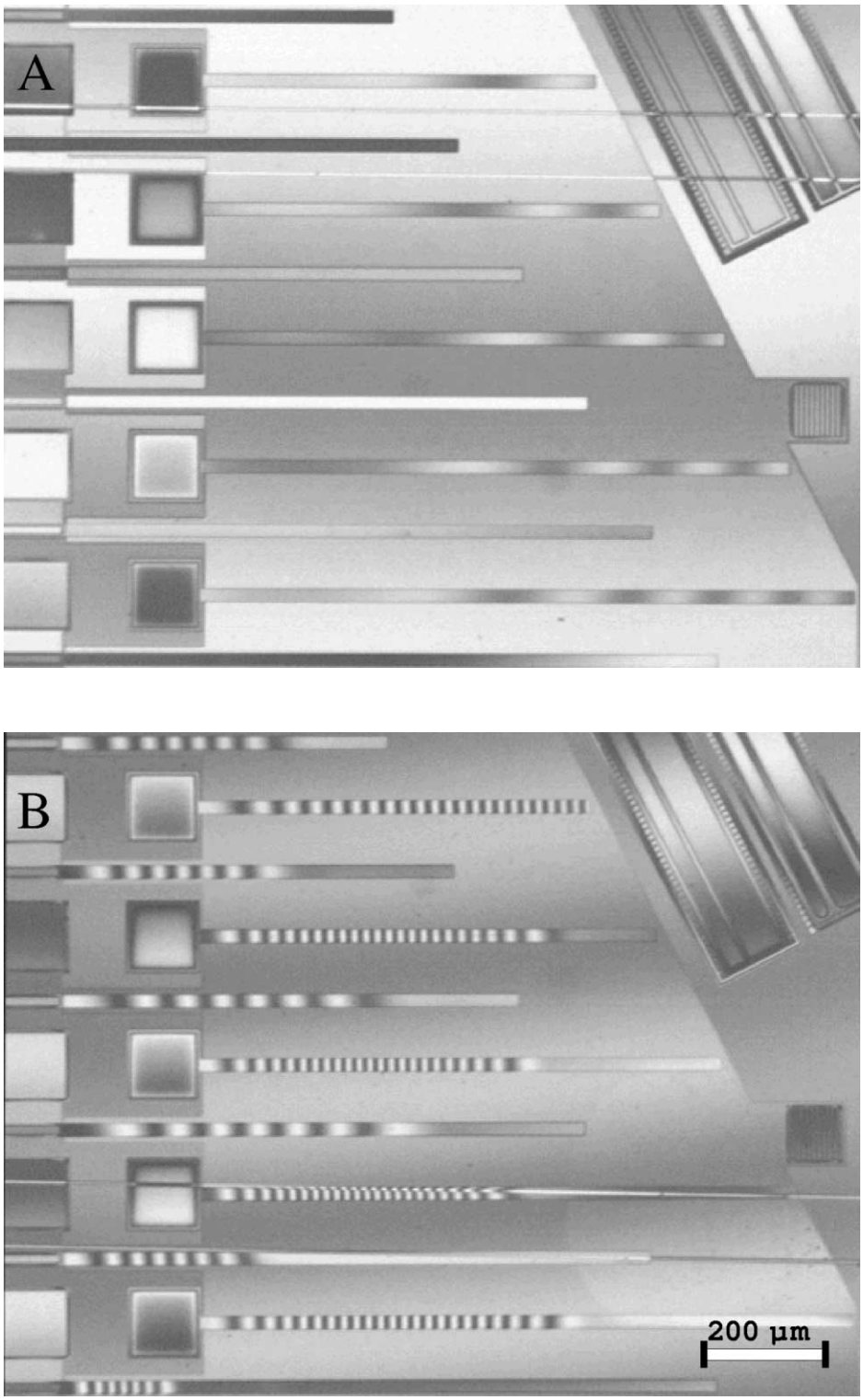

Figure 1. Beam release results for FDTS-covered test structures showing that both low stiction (A) and high stiction (B) can occur due to batch–batch variations in the coating.

When there is a monolayer or low percentage of surface aggregates, there is a low adhesion energy and release stiction is reduced. When the aggregate area increases to above 10% there are large adhesion forces and a high degree of beam stiction.

3.3. Water contact angle measurements

Although it is clear that the appearance of FDTS aggregates is correlated with release stiction, the test beam results do not reveal why the aggregates create adhesion problems.

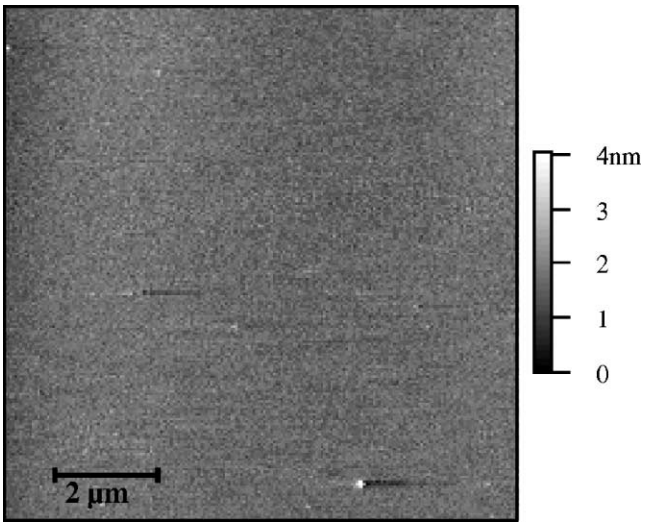

(A)

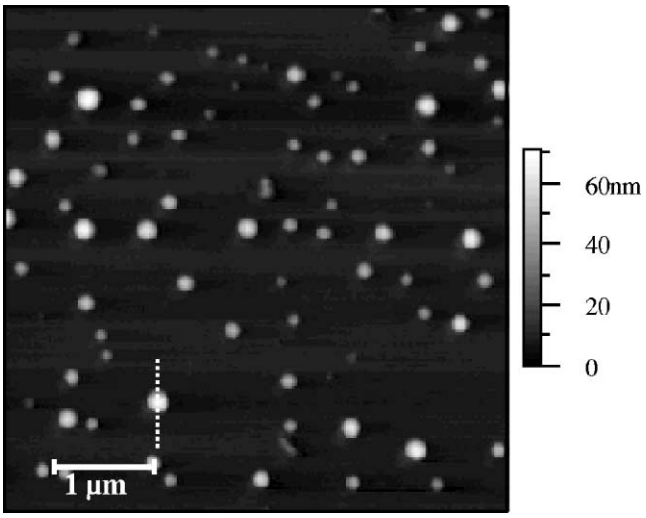

(B)

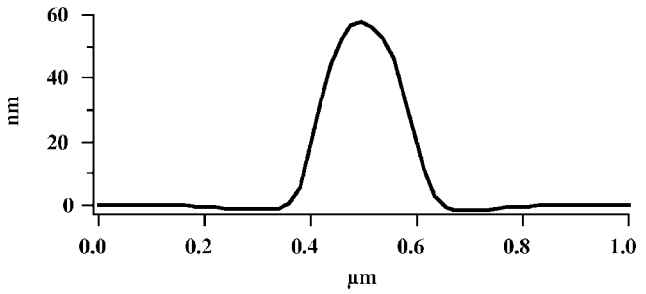

(C)

Figure 2. Tapping mode AFM image of a monolayer deposition of FDTS on a Si wafer (A). AFM image of an aggregate deposition of FDTS on a Si wafer (B). Line scan across FDTS aggregate (C).

The most obvious explanation for the results is that aggregates make beam surfaces more hydrophilic, either by being organized in such a way as to terminate surfaces with water or silanol head groups, or by scavenging FDTS to form hydrophilic bare patches in the underlying monolayer film.

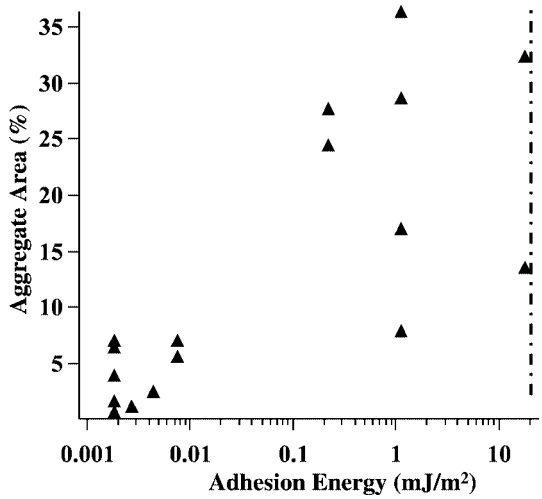

Figure 3. Plot of aggregate area versus adhesion energy for test structures coated with FDTS. Monolayer coatings of FDTS result in low adhesion energies and no release stiction. At aggregate densities above 10% adhesion increases dramatically with up to a four orders of magnitude more adhesion as compared to monolayer films. The vertical line represents the adhesion energy of uncoated beam test structures from [13].

Since the hydrophilic character of the beam and substrate are critical to controlling adhesion, we performed contact angle measurements to help quantify the extent to which the morphology of the coating influences surface free energies.

Release stiction is thought to result from the capillary forces exerted by water during the drying process. Underneath the microstructures, the water meniscus creates a Laplace pressure given by

$$P_{\mathrm{L}} = \frac{2\gamma\cos\theta}{d},$$

where the γ is the surface tension of water, θ is the water contact angle (assumed to be identical on both contacting surfaces), and d is the distance between the surfaces [14]. According to this equation, attractive interactions leading to stiction should only occur for contact angles of less than 90°. Since contact angles expected for dense FDTS coatings should be greater than 110°, this means that release stiction should not occur provided that the FDTS surfaces are completely terminated by fluorocarbon surfaces. In fact, over 30% of the surface would have to be covered by patches of hydrolyzed head groups (in micellar agglomerates) or by bare SiO_2 (the thermal oxide on Si) in order to lower the contact angle to the point where stiction might occur (assuming that the net contact angle is a population weighted average of the component contact angles) [15].

Water contact angle measurements were performed on Si wafers coated with either FDTS monolayers or inverse micelle aggregates to determine if the presence of aggregate structures generates a more hydrophilic surface (table 1). On average, monolayer films exhibit an advancing contact angle of 110°, which is close to the value of 115° expected for a fully dense fluorocarbon monolayer [3]. The receding contact angle is high (101°), and the hysteresis in contact angle ($\Delta\cos\theta$) is low, as expected. However, surfaces with high

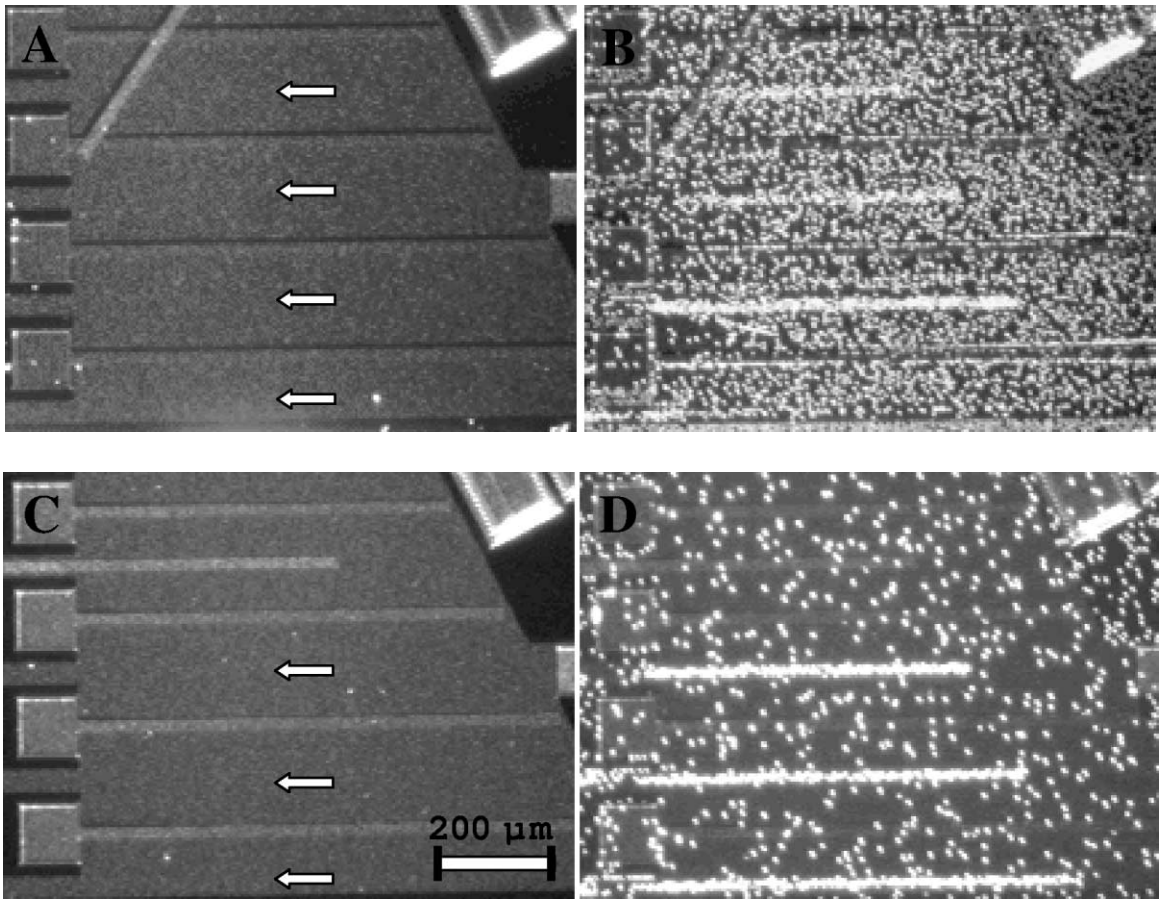

Figure 4. Optical micrographs and condensation figures of a monolayer (A and B) and aggregate (C and D) deposition of FDTS. Note the preferential condensation of water under the beams for the aggregate deposition (D) indicating a higher hydrophilicity for this area.

Table 1
Contact angles measured on FDTS films on Si.[a]

Film morphology	θ_a	θ_r	$\Delta \cos\theta$[b]
Monolayer	110 ± 4	101 ± 4	0.15 ± 0.02
Aggregate	115 ± 2	96 ± 3	0.32 ± 0.05

[a] Advancing (θ_a) and receding (θ_r) static contact angles of water.
[b] Contact angle hysteresis $\Delta \cos\theta = \cos\theta_r - \cos\theta_a$.

concentrations of the surface aggregates exhibit even higher advancing contact angles (115°) with a slightly higher contact angle hysteresis than the monolayer films. The presence of agglomerates does not appear to be accompanied by the formation of hydrophilic regions, at least on bare Si(100). Rather, the observed increases in contact angle and contact angle hysteresis can be attributed to increases in surface roughness associated with the aggregates [16]. The receding contact angle, which is the important parameter during drying, is always greater than 90° indicating that there should not be an attractive Laplace pressure or any release stiction between FDTS-coated parts, even when high concentrations of surface aggregates are present.

3.4. Condensation figure results

The discrepancy between the contact angle results and the fact that release stiction is observed for parts coated with aggregates suggests that the FDTS coatings are behaving differently on the polysilicon test beams than they behave on exposed Si wafers. One possible explanation for the discrepancy is that the aggregates in the deposition solution not only coat surfaces, but can form aggregate networks that bridge the 2 or 6 μm gap between the beams and the underlying substrate. (Individual aggregates are too small to bridge the gap.) Alternatively, the assumption that FDTS coating solutions form identical coatings on all surfaces (e.g., even under beams) may not be valid. To check the latter possibility, beams were physically removed after the coating procedure, and surfaces were examined using condensation figures.

Condensation figures (CFs) provide images of surface heterogeneities based on the decoration of features via the nucleation and growth of water droplets from supersaturated air. Whitesides and coworkers have demonstrated that water preferentially condenses on hydrophilic areas of patterned SAMs, providing a sensitive probe of differences in interfacial free energies between localized areas [17].

CFs obtained on FDTS-coated test structures after beam removal suggest that the FDTS is not as effective at producing hydrophobic surfaces under beams as it is on exposed surfaces. While it is not possible to detect where beams were in optical micrographs (figure 4 (A) and (C)), the regions that were under beams are readily observable after the

same substrates are exposed to supersaturated air to create condensation figures (figure 4 (B) and (D)). More water condenses on regions that were covered by beams. The contrast between regions that were or were not covered by beams during the deposition is much higher on surfaces containing the aggregates (figure 4(D)) than it is for monolayer films (figure 4(B)). The CF results suggest that regardless of coating structure, less FDTS is deposited under beams than on more exposed surfaces, resulting in a decrease in contact angle (an increase in hydrophilic character). Micellar aggregates appear to accentuate the effect by preventing more FDTS from getting under the beams, either by scavenging FDTS monomers or by interfering with surface diffusion. The condensation figure results are consistent with the test beam results (figure 3), which indicate that films with high aggregate concentrations approach the adhesion energy of uncoated beams (shown in the graph by the vertical line). Experiments are in progress to check this hypothesis by: (a) using scanning time-of-flight SIMS to measure FDTS surface concentrations, and (b) using an interfacial force microscope to probe adhesive interactions in regions that were and were not covered by beams during the deposition of both monolayer and agglomerate structures.

4. Conclusions

We have clearly shown that the film morphology dictates the anti-stiction properties of FDTS coatings. Release stiction is not observed when ideal monolayer films are present, but can be extensive when thicker aggregate structures are present. This finding is significant because it indicates that agglomerate formation during processing is a major source of irreproducible behavior when FDTS coatings are used to release micromachined parts. The results could also help explain why coatings that are aged at high humidity start to stick to each other. (AFM results show that humid environments promote the formation of aggregates from monolayer films [7].) The reason why aggregate structures promote stiction is currently unknown. However, it appears that aggregates interfere with the ability of FDTS to form dense, well-ordered coatings under microstructures, leading to surfaces that are sufficiently hydrophilic to allow for release stiction via an attractive Laplace force during drying.

Acknowledgement

This work was supported by Laboratory Directed Research and Development funds at Sandia National Laboratories. Sandia is a multiprogram laboratory operated by Sandia Corporation, a Lockheed Martin Company, for the United States Department of Energy under contract DE-AC04-94AL85000. JGK would like to thank W.L. Smith for help in constructing the contact angle apparatus.

References

[1] C.H. Mastrangelo and C.H. Hsu, J. MEMS 2 (1993) 33.
[2] R. Maboudian and R.T. Howe, J. Vac. Sci. Technol. B 15 (1997) 1.
[3] R. Maboudian, W.R. Ashurst and C. Carraro, Sens. Actuators A 82 (2000) 219.
[4] A.N. Parikh, D.L. Allara, I.B. Azouz and F. Rondelez, J. Phys. Chem. 98 (1994) 7577.
[5] B.C. Bunker, R.W. Carpick, R.A. Assink, M.L. Thomas, M.G. Hankins, J.A. Voigt, D.L. Sipola, M.P. de Boer and G.L. Gulley, Langmuir 16 (2000) 7742.
[6] A.N. Parikh, M.A. Schivley, E. Koo, K. Seshadri, D. Aurentz, K. Mueller and D.L. Allara, J. Am. Chem. Soc. 119 (1997) 3135.
[7] M.P. de Boer, T.M. Mayer, R.W. Carpick, T.A. Michalske, U. Srinivasan and R. Maboudian, submitted.
[8] J.J. Sniegowski and M.P. de Boer, Annu. Rev. Mater. Sci. 30 (2000) 297.
[9] M.P. de Boer and T.A. Michalske, J. Appl. Phys. 86 (1999) 817.
[10] P.E. Laibinis, G.M. Whitesides, D.L. Allara, Y.T. Tao, A.N. Parikh and R.G. Nuzzo, J. Am. Chem. Soc. 113 (1991) 7152.
[11] A.W. Neumann and J.K. Spelt, *Applied Surface Thermodynamics* (Dekker, New York, 1996).
[12] M.P. de Boer and T.A. Michalske, Mater. Res. Soc. Symp. Proc. 444 (1997) 87.
[13] M.R. Houston, R. Maboudian and R.T. Howe, Hilton Head '96, Hilton Head Island, SC (3–6 June 1996) 42.
[14] R. Maboudian, Surf. Sci. Rep. 30 (1998) 209.
[15] J. Drelich, J.L. Wilbur, J.D. Miller and G.M. Whitesides, Langmuir 12 (1996) 1913.
[16] J.N. Israelachvili, *Intermolecular & Surface Forces* (Academic Press, New York, 1991).
[17] G.P. Lopez, H.A. Biebuyck, C.D. Frisbie and G.M. Whitesides, Science 260 (1993) 647.